Eur. Phys. J. D **30**, 441–444 (2004)
DOI: 10.1140/epjd/e2004-00096-0

THE EUROPEAN PHYSICAL JOURNAL D

Evolution of photoelectron angular distributions in a train of identical, circularly polarized few-cycle laser pulses

J.T. Zhang[1,2,a], S.H. Li[2,3], and Z.Z. Xu[2]

[1] CCAST (World Laboratary), P.O. Box 8730, Beijing 100080, P.R. China
[2] Laboratory for High Intensity Optics, Shanghai Institute of Optical and Fine Mechanics, Chinese Academy of Sciences, Shanghai 201800, P.R. China
[3] Department of Physics, Shantou University, Shantou 515063, P.R. China

Received 18 November 2003 / Received in final form 26 February 2004
Published online 10 August 2004 –

Abstract. Photoelectron angular distribution (PAD) of atoms irradiated by a train of identical, circularly polarized few-cycle laser pulses is studied in the frame of a nonperturbative scattering theory. Our study shows that the PADs vary with the kinetic energy of photoelectron, the carrier-envelope phase, and the pulse duration. We find that along with increasing of the kinetic energy of photoelectron or with decreasing of the pulse duration or the both, the original one maximum of PAD splits into two maxima; the newly produced two maxima evolve to the opposite pole of the symmetric axis, and finally incorporate as a new maximum located in the symmetric axis.

PACS. 32.80.Rm Multiphoton ionization and excitation to highly excited states (e.g., Rydberg states) – 42.50.Hz Strong-field excitation of optical transitions in quantum systems; multiphoton processes; dynamic Stark shift – 42.65.Re Ultrafast processes; optical pulse generation and pulse compression

Recent developments in laser technology have made it possible to produce high intensity laser pulse of few optical cycles [1], which provide a useful tool in various fields [2,3]. For a few-cycle pulse, the temporal shape of its electric field varies dramatically with the value of the initial phase of the carrier wave with respect to the envelope. All physical processes induced by such a field depend on the carrier-envelope (CE) phase, for example, the emitted electrons in above-threshold ionization (ATI) [4,5].

When atoms are irradiated by intense laser pulses, the photoelectrons are produced at a rate determined by the instantaneous electric field. If atoms are irradiated by long, single-color laser pulses, the photoelectrons rates in a pair of two opposite directions are always identical, thus the photoelectron angular distributions (PADs) show the inversion symmetry [6]. While, if atoms are irradiated by short pulses, the photoelectron rates in a pair of two opposite directions are not always equal to each other, thus the PADs are inversion asymmetric. Because the amplitude of the electric field varies smoothly with time, the use of circularly polarized pluses is beneficial [7]. It has been shown that the PADs in circularly polarized few-cycle pulse is not isotropic, and that the position of the maximum of PADs varies with the CE phase and the pulse duration [8]. Here, the pulse duration denotes the number of optical cycles in a single pulse. Since the value of the CE phase determines the distribution of the electric field in the pulse, it is easy to see the reason why the CE phase affects the PADs. However, how the pulse duration to influence the PADs is still an open problem. In this paper, we present a solution to this problem.

The photoionization in circularly polarized few-cycle laser pulses was firstly studied by means of a classical method, and the variation of the angular distribution with the CE phase, the laser intensity and the pulse duration were shown [7]. The present paper focuses on the variation of the PADs with the pulse duration and the kinetic energy of photoelectrons in the frame of a nonperturbative quantum theory of ATI developed by Guo et al. [9]. In this theory, the final state of ATI is treated as an electron-photon plane wave while the Volkov states as intermediate states. The Volkov state describes a free electron moving in a laser plane wave [10], thus, when we use Volkov states, two points should be mentioned. First, the Coulomb attraction of the parent ion to the ionized electron is neglected, which is the strong-field approximation widely used in intense laser studies [11]; second, the few-cycle pulses can be treated as a combination of plane waves and a three-mode laser is used to mimic a train of identical few-cycle pulses [8].

This study is an extension of our earlier study, which focused on the inversion symmetry and the CE-dependence of the PADs when atoms are exposed to a

[a] e-mail: jtzhang@siom.ac.cn

sequence of short pulses. In this paper, we present the variation of the PADs with the pulse duration and the kinetic energy of electron. A three-mode laser field is used to mimic a long sequence of identical few-cycle pulses. Details are presented in reference [8]. The state of a nonrelativistic electron in the few-cycle pulses is described by [12]:

$$|\Psi_\mu\rangle = V_e^{-1/2} \sum_{j_1,j_2,j_3} \exp\{i[\mathbf{P} + (u_{p1} - j_1)\mathbf{k}_1 + (u_{p2} - j_2)\mathbf{k}_2 + (u_{p3} - j_3)\mathbf{k}_3] \cdot \mathbf{r}\} \times \mathcal{X}_{j_1,j_2,j_3}(z)|n_1 + j_1, n_2 + j_2, n_3 + j_3\rangle, \quad (1)$$

where $\mathbf{P}$ is the momentum of photoelectron inside the field, m_e is the electron rest mass, and V_e is the electron normalization volume; $\mathbf{k}_i = \omega_i \mathbf{k}_0$ is the wave vector of each mode with $\mathbf{k}_0$ being the unit vector along the pulse propagation direction; $|n_i + j_i\rangle$ $(i = 1, 2, 3)$ is the Fock state of the ith mode with n_i being the number of background photons in this mode, the sum over the transferred photon j_i is performed over $-n_i \leqq j_i < \infty$, and u_{pi} is the ponderomotive parameter of the ith mode defined as

$$u_{pi} = \frac{e^2 \Lambda_i^2}{m_e \omega_i}, \qquad (i = 1, 2, 3)$$

in which $2\Lambda_i$ is the amplitude of the ith classical field, and

$$\omega_1 = \omega, \ \omega_2 = \omega(1 + 1/n), \ \ \omega_3 = \omega(1 - 1/n), \quad (2)$$

where ω is the circular frequency of the carrier wave and n is the number of cycles included in a single pulse, which relates to the pulse duration τ as $\tau = 2n\pi/\omega$. In the Volkov state, the generalized phased Bessel (GPB) function for circularly polarized laser field is given by

$$\mathcal{X}_{j_1,j_2,j_3}(z) = \sum_{m_1,m_2,m_3} X_{-j_1+m_1+m_2}(\zeta_1) \times X_{-j_2-m_2+m_3}(\zeta_2) X_{-j_3-m_2-m_3}(\zeta_3) \times X_{-m_1}(z_1) X_{-m_2}(z_2) X_{-m_3}(z_3), \quad (3)$$

where the sum is performed over $-\infty < m_i < \infty$, and $X_n(z)$ is the phased Bessel function related to the ordinary Bessel function as

$$X_n(z) = J_n(|z|) e^{in \arg(z)}.$$

The arguments of the GPB function are defined as

$$\zeta_1 = \frac{2|e|\Lambda_1}{m_e\omega_1}\mathbf{P} \cdot \epsilon_1, \qquad \zeta_2 = \frac{2|e|\Lambda_2}{m_e\omega_2}\mathbf{P} \cdot \epsilon_2,$$
$$\zeta_3 = \frac{2|e|\Lambda_3}{m_e\omega_3}\mathbf{P} \cdot \epsilon_3, \qquad z_1 = \frac{2e^2\Lambda_1\Lambda_2\epsilon_1 \cdot \epsilon_2^*}{m_e(\omega_2 - \omega_1)},$$
$$z_2 = \frac{2e^2\Lambda_1\Lambda_3\epsilon_1 \cdot \epsilon_3^*}{m_e(\omega_3 - \omega_1)}, \qquad z_3 = \frac{2e^2\Lambda_2\Lambda_3\epsilon_2 \cdot \epsilon_3^*}{m_e(\omega_3 - \omega_2)}, \quad (4)$$

where $\vec{\epsilon}_j$ is the polarization vector defined as

$$\epsilon_j = [\epsilon_x \cos(\xi/2) + i\epsilon_y \sin(\xi/2)] e^{i\phi_j},$$
$$\epsilon_j^* = [\epsilon_x \cos(\xi/2) - i\epsilon_y \sin(\xi/2)] e^{-i\phi_j}, \quad (5)$$

in which ϕ_j $(j = 1, 2, 3)$ is the phase angle of each mode

$$\phi_1 = \pi, \quad \phi_2 = -\phi_0/n, \quad \phi_3 = \phi_0/n,$$

with ϕ_0 being the CE phase, and ξ determines the degree of polarization, such that $\xi = \pi/2$ corresponds to the circular polarization.

By means of the Volkov state in equation (1), we get the differential transition rate for a given ATI peak as follows [8]

$$\frac{d^2W}{d\Omega_{p_f}} = \frac{(2m_e^3\omega^5)^{1/2}}{(2\pi)^2}(q - \epsilon_b)^{1/2}(q - 4u_{p1})^2 |\Phi_i(\mathbf{P}_f - q\mathbf{k}_1)|^2 \times \left| \sum_{q_i,j_i} \mathcal{X}_{j_1-q_1,j_2-q_2,j_3-q_3}(z_f) \mathcal{X}_{j_1,j_2,j_3}(z_f)^* \right|^2, \quad (6)$$

where $\Phi_i(\mathbf{P}_f - q\mathbf{k}_1)$ is the Fourier transformation of the initial wave function with binding energy E_b, and $\epsilon_b = E_b/\omega$ is the binding number; $q_i = l_i - m_i$ $(i = 1, 2, 3)$ is the overall transferred photon number in the ith mode during the interaction, and we use

$$q = [q_1\omega_1 + q_2\omega_2 + q_3\omega_3]/\omega \quad (7)$$

to denote an ATI peak, since it determines the final kinetic energy of the emitted electrons. The sum over q_i is performed over all possible q_1, q_2 and q_3 for a fixed q. The argument z_f in equation (6) means that the $\mathbf{P}$ in equation (4) is replaced by $\mathbf{P}_f$ while others are kept unchanged. Here, $\mathbf{P}_f$ is the final momentum of the photoelectron. The emission rate of a given ATI peak is got by integrating over the solid angle, and the PADs denotes the emission rate at a fixed scattering angle θ_f for various azimuth ϕ_f.

By means of the transition-rate formula in equation (6), we obtain the angular distribution of the ejected electrons. We choose Kr as the sample atoms in the calculation, of which the outermost shell is $4P_{3/2}$ with binding energy 13.99 eV. The laser pulses are of circular polarization, central wavelength 800 nm, and peak intensity $I = 5 \times 10^{13}$ W/cm^2.

Our calculations show that in long-pulse cases, the PADs in circularly polarized laser light are azimuthal isotropic, which agrees with earlier studies [6]; and that the PADs in few-cycle pulses are not isotropic and the photoelectron rates in a pair of two opposite directions are not always equal to each other, which is termed as inversion asymmetry. The inversion asymmetry with respect to the space reflection is caused by the interference effect among different transition channels, where different channels are characterized by different combinations of absorbed-photon numbers in the ionization process [8]. For circularly polarized few-cycle pulses, the maximal strength of the electric field keeps constant for different CE phases, but its position varies with the value of CE phase. As a result, the maximal emission rate keeps constant, but its position varies with the CE phase. Due to the symmetry of the electric field with respect to its maximum, the PADs are symmetric about an axis related to the CE phase. The

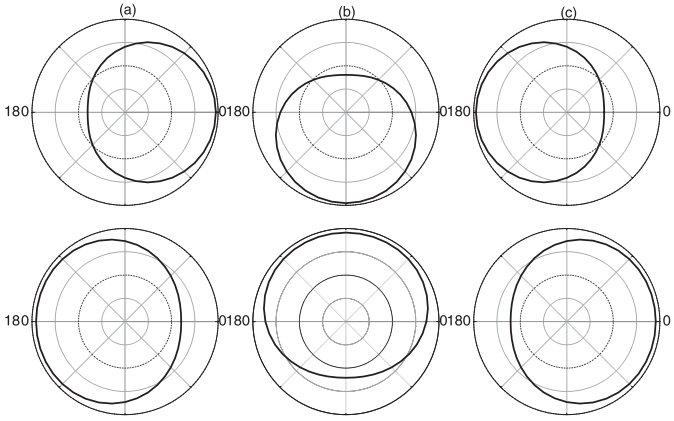

Fig. 1. Polar plots of the calculated PADs of the 1st (the top row) and the 5th (the bottom row) ATI peaks for several CE phases for 5–cycle pulses: (a) $\phi_0 = 0°$, (b) $\phi_0 = 90°$, and (c) $\phi_0 = 180°$. The laser is circularly polarized at wavelength 800 nm and intensity $I = 5 \times 10^{13}$ W/cm^2. The maxima and the symmetric axis of PADs rotate with the value of CE phase and show the dependence of PADs on the CE phase. Comparison between the top row and the bottom row discloses the dependence of PADs on the ATI orders.

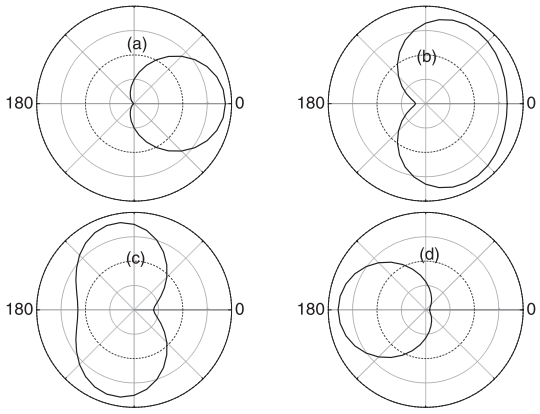

Fig. 2. Polar plots of the calculated PADs when $\phi_0 = 0°$ and $n = 5$ for (a) 6th, (b) 7th, (c) 8th, and (d) 9th ATI peaks. Other conditions are the same as those in Figure 1.

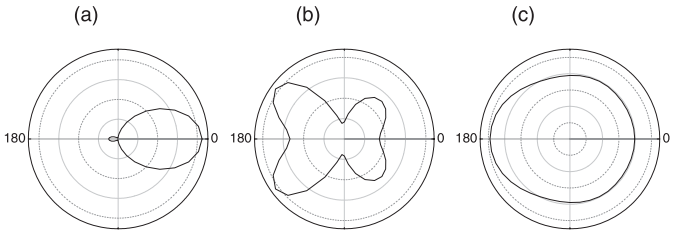

Fig. 3. Polar plots of the calculated PADs when $\phi_0 = 0°$ and $n = 2$ for (a) 4th, (b) 5th, and (c) 6th ATI peaks. Other conditions are the same as those in Figure 1.

variation of the PADs on the CE phase are shown in Figure 1 for the 1st and the 5th ATI peaks when $n = 5$.

The CE phase is not the unique factor that determines the characters of PADs. The position of the extrema of PADs also varies with the duration of a single pulse. Take the first ATI peak for $\phi_0 = 0°$ as an example. For a 5–cycle pulse, the maximum of the PAD locates at $\phi_f = 0°$, but locates at $\phi_f = 180°$ for a 3–cycle pulse. Additionally, the position of the maximum of the PADs varies with the order of ATI peaks. For example, in a 5−cycle pulse, the maxima of the PADs of the 1st and the 5th peaks locate in the opposite direction in the symmetric axis for the same CE phase, as shown in Figure 1. The difference in the position of the maximal emission rate, for the same pulse duration and for the same CE phase, discloses that the maximal ionization is not always corresponding to the maximum of the electric field, although the photoelectrons are produced at a rate related to the electric field strength. Furthermore, the PADs of some ATI peaks split with the maxima located far off the symmetric axis, thus shows another kind of unexpected structures.

The splitting in PADs appears for different ATI peaks and for different pulse durations, but whether the splitting appears or not has no relation with the CE phase. Generally, only the PADs of higher order ATI peaks exhibit the splitting for longer pulses, while for shorter pulses, even the PADs of lower order ATI peaks show the splitting. For example, for 4–cycle pulses, the splitting first appears in the PAD of the 5th ATI peaks, and other low order peaks show no splitting in PADs; but for 2–cycle pulses, the PADs of the 1st and the 2nd peaks show the splitting, while the PAD of the 3rd peak shows only subtle splitting, and no splitting appears in the PAD of the 4th peak. Some results are shown in Figures 2 and 3.

The unexpected structures were frequently observed in experiments, such as the ring structure in high order ATI peaks [13] and the jet structure in low order ATI peaks [14–17]. These unexpected structures are related to the order of ATI peak q, the ponderomotive parameter u_p, and the binding number ϵ_b. The jet structure are caused by the maxima of the GPB function and the total number of jets in one side of PADs is twice the number of the maxima in the domain of $\zeta-$variable [18]. This result is suggestive to the present study. Different ATI peaks mean different kinetic energy of the photoelectron, which affects, in turn, the ζ-variables and the orders of the GPB functions, the values of the GPB functions, the emission rate in a single channel, and finally the PADs. The pulse duration, denoted by n, affects PADs through three factors: the channel number, the phase of each transition channel, and the transition rate of each channel. The dependence of channel number on the pulse duration is easily got from equations (2) and (7), and more channels are involved to form an ATI peak for a shorter pulse. The phase of each channel varies with the pulse duration in a manner as $(q_2 - q_3)\phi_0/n$, which indicates that different pulse durations affect the interference pattern among transition channels. The pulse duration affects the arguments of the GPB function through the frequencies ω_i and the ponderomotive parameters u_{pi} $(i = 2, 3)$, and finally affects the ionization rate in each channel. The pulse duration shows its influence via these three factors, but the

last one is the leading factor. Keeping other conditions unchanged, shorter pulse durations lead to larger ζ_3 and ζ_2. An equivalent situation occurs for higher order ATI peaks at a longer pulse duration, thus the PADs for lower order peaks in shorter pulses show similar splitting to those for higher order peaks in longer pulses, which is clear after a comparison made between Figures 2 and 3. That shorter pulse durations lead to larger variables of the GPB functions reflects the fact that a higher effective field strength is reached in shorter pulses.

The splitting in PADs discloses the inherent properties of the photoionization process and reveals an evolution of maximal emission rate along with the ATI orders and the pulse durations. Before and after the splitting, the positions of the maxima of PADs are in the opposite directions of the symmetric axis of the PADs. For example, when $\phi_0 = 0^\circ$ in a 5−cycle pulse, the maximal emission of the 6th peak is located at $\phi_f = 180^\circ$, but that of the 9th peak is at $\phi_f = 0^\circ$, in the between, the PADs split. Similar phenomena occur for other peaks at different pulse durations, as shown in Figures 2 and 3. Thus, one can reach a uniform view point to the evolution of PADs: the anisotropic PAD has a maximum located at one pole of the symmetric axis. Along with the increasing arguments, induced by the shortening of pulse durations or the increase of ATI orders or the both, the PAD shows a splitting: the original one maximum splits into two maxima symmetrically located at two sides of the symmetric axis; the newly produced two maxima evolve to the opposite pole of the symmetric axis. When the two maxima meet in the symmetric axis, they incorporate as a new one. Then the PAD experiences a whole evolution, with the new maximum located at the opposite pole of the symmetric axis to the original one. During the evolution, the dependence of PADs on the CE phase still holds, since the CE phase doesn't change the domain of the arguments of the GPB functions.

In our three-mode treatment, the few-cycle laser pulses are not a single pulse but a train of identical few-cycle pulses irradiating the target atoms one by one. This corresponds to the few-cycle pulses with fixed CE phase produced by high repetition lasers. The splitting in the PADs arises from the inherent properties of ATI, and has no relation to the three-mode treatment. If the CE phase of the short pulses can be fixed in a small range, the predicted phenomena will be observed experimentally. We notice that recent developments in laser technology have made it possible to produce few-cycle pulses with CE phase variation less than 0.1π, the predicted PADs are expected to be observed experimentally in the near future.

This work is supported by the National Natural Science Foundation of China under Grant Nos. 60178014 and 10234030, and National Key Basic Special Research Foundation under Grant No. G1999075200.

References

1. M. Nisoli, S. De Silvestri, O. Svelto, R. Szipcs, K. Ferencz, Ch. Spielmann, S. Satrania, F. Krausz, Opt. Lett. **22**, 522 (1997)
2. T. Brabec, F. Krausz, Rev. Mod. Phys. **72**, 545 (2000)
3. A. Baltuska et al., Nature **421**, 611 (2003)
4. G.G. Paulus, F. Grasbon, H. Walther, P. Villoresi, M. Nisoli, S. Stagira, E. Priori, S. De Silvestri, Nature **414**, 182 (2001); D.B. Milosevic, G.G. Paulus, W. Becker, Phys. Rev. Lett. **89**, 153001 (2002)
5. H.M. Nilsen, L.B. Madsen, J.P. Hansen, Phys. Rev. A **66**, 025402 (2002); J.P. Hansen, J. Lu, L.B. Madsen, H.M. Nilsen, Phys. Rev. A **64**, 033418 (2001)
6. M. Bashkansky, P.H. Bucksbaum, D.W. Schumacker, Phys. Rev. Lett. **60**, 2458 (1988); Phys. Rev. Lett. **59**, 274 (1987); P. Krstic, M.H. Mittleman, Phys. Rev. A **44**, 5938 (1991)
7. P. Dietrich, F. Krausz, P.B. Corkum, Opt. Lett. **25**, 16 (2000)
8. J. Zhang, Z. Xu, Phys. Rev. A **68**, 013402 (2003)
9. D.-S. Guo, T. Aberg, B. Crasemann, Phys. Rev. A **40**, 4997 (1989)
10. D.-S. Guo, T. Aberg, J. Phys. A **21**, 4577 (1988)
11. M. Lewenstein, Ph. Balcou, M. Yu. Ivanov, A. L'Huillier, P.B. Corkum, Phys. Rev. A **49**, 2117 (1994)
12. D.-S. Guo, G.W. Drake, J. Phys. A **25**, 5377 (1992)
13. B. Yang, K.J. Schafer, B. Walker, K.C. Kulander, P. Agostini, L.F. Dimauro, Phys. Rev. Lett. **71**, 3770 (1993)
14. M.J. Nandor, M.A. Walker, L.D. van Woerkom, J. Phys. B **31**, 4617 (1998)
15. V. Schyja, T. Lang, H. Helm, Phys. Rev. A **57**, 3692 (1998)
16. G.D. Gillen, L.D. van Woerkom, Phys. Rev. A **68**, 033401 (2003)
17. R. Wiehle, B. Witzel, H. Helm, E. Comiern, Phys. Rev. A **67**, 063405 (2003)
18. J. Zhang, W. Zhang, Z. Xu, X. Li, P. Fu, D.-S. Guo, R.R. Freeman, J. Phys. B **35**, 4809 (2002)